Indonesian Journal of Earth Sciences, Vol. 3, No. 1 (2023), 609

P-ISSN: 2798-1134 | E-ISSN: 2797-3549 | DOI: 10.52562/injoes.2023.609

Indonesian Journal of Earth Sciences

https://journal.moripublishing.com/index.php/injoes

| Research Article |

# Geoinformatics Perspective of Landslide and Catastrophic Flash Floods in Dhauliganga, Uttarakhand, India

**Deepti Kumari Dwivedi [1]*, Arun Kumar Saraf [2], Josodhir Das [3]**

[1]*Centre of Excellence in Disaster Mitigation and Management, Indian Institute of Technology Roorkee, Uttarakhand, India*
[2]*Department of Earth Sciences, Indian Institute of Technology Roorkee, Uttarakhand, India*
[3]*Department of Earthquake Engineering, Indian Institute of Technology Roorkee, Uttarakhand, India*
** Correspondence: dwideepti@gmail.com*

Received: 01 April 2023 / Accepted: 05 May 2023 / Published: 08 May 2023

**Abstract:** On 07 February 2021, around 10:30 hrs local time catastrophic flash flood occurred in the Dhauliganga River (a tributary of the Ganga River) near Rini village at 2000 m above MSL (mean sea level) (Chamoli District), which killed 79 people and about 125 people were missing. Part of the area belongs to Nanda Devi Biosphere Reserve, which is completely protected from human interventions. Further, on the Dhauliganga River, two run-of-river hydroelectric power Rishiganga Small Hydro (13.2 MW) at 1975 m above MSL and Tapovan Vishnugad (520 MW) at 1795 m above MSL projects were also severely damaged due to the devastating flash flood. More than 150 workers were also trapped in the under-construction power tunnel of the Tapovan Vishnugad project. Initial assessment on the day of the event suggested that there was a glacial burst. Later, it was evaluated through time series of high spatial resolution remote sensing images of various satellites that a large part of a north-facing triangular-shaped slope at 5540 m above MSL had failed, which was also supporting a small hanging glacier. This landslide and, consequently, massive debris flow into the Raunthi Gadhera initially blocked the flow of Dhauliganga near Rini village [at 2000 m above MSL (mean sea level)], which later failed around 10:30 hrs on 07 February 2021 and brought a catastrophic flash flood in the Dhauliganga river. Further, remote sensing images acquired around 10:33 hrs of 07 February 2021 revealed a large dust cloud which clearly unravels the sequence of events from a high-altitude landslide, collapse of a small hanging glacier, and snow avalanche to catastrophic flooding. Even after the catastrophic flash flood of 07 February 2021, an elongated lake was created due to the blocking of the flow of the Rishi Ganga River. For detailed analysis, the calculation of dimension, area and volume of the failed slope was done using the high-resolution satellite images and digital elevation model using the RAMMS modelling technique. The north-facing triangular shape had a base of about 660 m and 1100 m height and the estimated total volume calculated was 20 million cubic meters, including rocks, snow, and ice. The debris flow runout simulation of the event was performed using the RAMMS debris flow model to calculate flow depth, flow velocity and maximum pressure. Also, from high-resolution satellite images, the dimensions of the artificial Rini Lake were estimated to have a length of about 800 m, a width at the front of about 100 m and a depth of about 46m, including freshly deposited debris and silt of about 10 m. To calculate the volume of the lake, simulation of lake was done in ArcView software using digital elevation model, and it came out to be ~5 million cubic meters. The paper also emphasizes monitoring of such vulnerable areas based on high-resolution time series satellite images, which are available on a regular basis to avoid the loss of human lives in the future.

**Keywords:** Spatial Resolution; Remote Sensing; Landslide; RAMMS

## INTRODUCTION

The Himalaya is a seismically highly active, rugged and fragile mountain system as it has formed from the collision between the Indian Plate and Eurasian Plate, which began about 50 million years ago and still continues. The Indian Himalayan region is highly susceptible to landslide incidents because of various factors like complex geology, rugged topography, and steep slopes also, triggered by heavy rainfall and frequent earthquake activities (Sarkar et al., 2016; Meena et al., 2019). The slopes in the higher Himalayas are generally very steep and consequently highly prone to landslides, leading to heavy loss of both life and property. Landslides-induced damming and later flash floods are inevitable disasters in the Himalayas. Moreover, the fragile nature of the Indian Himalayas and continuous anthropogenic activities in the natural landscape increases slope instability and lead to multiple hazards, which may be further subjected to climate change or extremes (Batar & Watanabe, 2021). Besides landslides, snow avalanche is commonly observed in this region in which changes in surface and subsurface ice, especially in combination with unfavorable geological conditions, can reduce the strength of rock and ice and destabilize slopes, thus leading to slope failures such as rock and snow avalanches (Haeberli et al., 1997; Davies et al., 2001). Observations of such slope failures in mountain regions suggest that slope stability problems in steep high-mountain faces are of significant concern in view of ongoing climate changes and the hazard potential they possess (Evans & Clague, 1994; Geertsema et al., 2006; Oppikofer et al., 2008; Allen et al., 2011; Fischer et al., 2012).

Uttarakhand, the Himalayan state, is located between 28° 43' - 31° 27' N latitude and 77° 34' - 81° 02' E longitude having 13 districts and is divided into two geographical regions i.e. Kumaon and Garhwal. The fragile ecosystem, tectonic set-up and high precipitation along with cloudbursts and the vested interests of people in real estate, increased number of tourist in eco-sensitive regions, unscientific methods of land use and waste disposals, as well as the construction of mega hydropower projects leads to the occurrence of many hazards (Kala, 2011). Natural disasters like Himalayan tsunamis, flash floods, earthquakes, landslides, hailstorms, cloudbursts, snow avalanches, soil erosion and forest fire are mostly occurred hazards in Uttarakhand, causing loss of lives and property; however, the most prevalent disaster in the state is the landslide. Some historical landslides in the state are the Gohna landslide which occurred in 1893 (Dwivedi et al., 2023), numerous landslides which were triggered after the flash floods of 20 July 1970 in the Alaknanda River and the most disastrous Kedarnath landslide, which took place in June 2013 (Kala, 2014).

The present study emphasizes on the recent landslide event which occurred in the Chamoli district of the Uttarakhand state, which then led to the catastrophic flash floods. The objective of this study is to have a detailed analysis of the event, starting from the triggering of the event to the ice avalanche breakoff, failure of the triangular wedge, damming, formation of the artificial lake, the debris flow and finally, the damages caused by the event. The various estimations and calculations of the area/volume of the wedge and the Rini lake have been done by using high-resolution satellite images and different modelling techniques like the RAMMS model and ArcView software. The simulation of the artificially formed lake and the whole event was also performed. Satellite images of recent years (2016-17) have also revealed that there were many such incidences of slope failures in the Rishiganga Valley but they went unnoticed because these events did not generate devastating flash floods.

## MATERIALS AND METHODS

### Study Area

Rishiganga Valley is located in the Chamoli district, Uttarakhand, India, which lies in the central Himalayas. Rishiganga River springs from the Uttari Nanda Devi Glacier on the Nanda Devi Mountain flows in the Rishiganga valley, and it is also fed from the Dakshini Nanda Devi Glacier. Continuing through the Nanda Devi National Park, it flows into the Dhauliganga River near the village Rini. Raunthi Gadhera (Ronti Gad) is a tributary of the Rishiganga River, which later meets the Dhauliganga River near Rini (Reni) village (Fig. 1). This area falls under the category of severe earthquake zone and during the last thirty years the region has also witnessed about 53 earthquakes (within 100 km) of magnitude ranging $M_w$ 3.2–6.6 (Fig. 2). Also, the study area belongs to very high to severe category in landslide hazard zonation map of Uttarakhand (Pant & Pande, 2012). Moreover, a large part of Rishiganga Valley having very steep slopes (Sangeeta & Maheshwari, 2019) and is covered with glacial moraine sediments and therefore due to availability of abundant loose sediments there are always possibilities of damming of streams and consequently flash floods in the event of natural dam failure.

### Materials Used

Precipitation (snow and rain) data from Automatic Weather Station, Tapovan, is obtained to get the details of precipitation for seven days (1st to 7th February 2021). Pre- and post-disaster high-resolution satellite datasets used in the present study are from Planet Scope from PLANET, Indian Remote Sensing Satellite Constellation (Resourcesat-2 and Cartosat2A) from ISRO, Sentinel-2A from European Space Agency and Pleaides from CNES (Space Agency of France), Google Earth Images, these are collected from different sources. Digital Elevation Model of 10 m spatial resolution Cartosat, SRTM DEM of 30 m spatial resolution and WorldView-1 Stereo DEM of 2 m spatial resolution are used for the simulation using ArcView and RAMMS (rapid mass movement simulation) model.

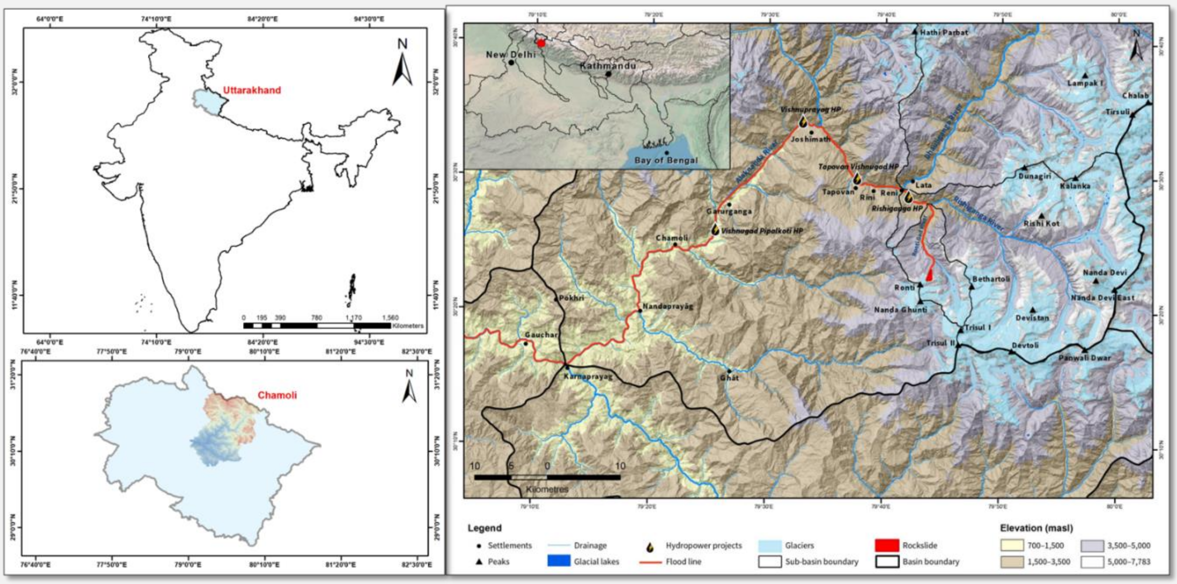

Figure 1. Depicts landslide / rockslide origin and flash flood path along the Raunthi Gadhera, Rishiganga and Dhauliganga Rivers (Shrestha et. al., 2021)

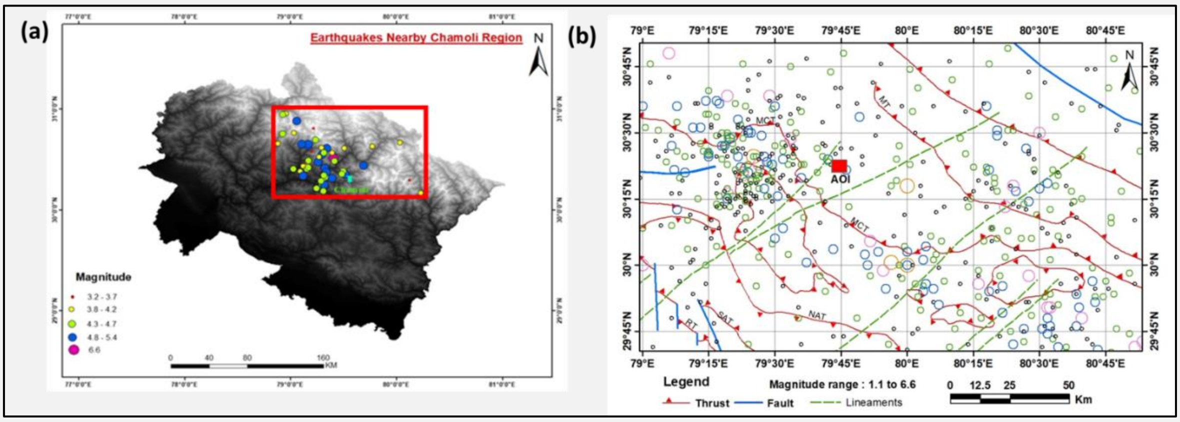

Figure 2. Earthquakes occurred (within 100 km) in the region during 1990-2021. The pink-coloured filled circle depicts the Chamoli Earthquake of 29 March 1999, 6.6 $M_w$ (a); Map showing thrust, fault and lineaments near the area of interest (Ronti gad) marked with a red rectangle (b)

## Methodology

The methodology used in the present study uses two different remote sensing datasets (Fig. 3). The first dataset is multi-temporal and high-resolution satellite images, and the second dataset is Digital Elevation Model. The high-resolution satellite images are used to study the sequence of the event, damage assessment and also a similar type of past case study which occurred in October 2016 in the same area. High spatial resolution satellite images (Pre-post event) to observe the cause of the event and also to observe the changes caused by the event Pseudo Colour Technique is used. The conventional PCT technique facilitates the combination of various bands in different colour schemes, such as RGB, IHS and CMY. However, instead of using the different bands of the same date data, an approach developed by Saraf (1998) has been adopted in the present study to map the landslides/rockslide-induced ground changes using available high-resolution pre- and post-event datasets of the Pléiades satellite. Later Google Earth images are used to assess the damage caused by the event and also to study a similar type of event which occurred in September-October 2016 over the same region.

The second dataset, Digital Elevation Models of different spatial resolutions, is used for the simulation of Rini Lake and the whole event. Simulation of Rini Lake using ArcView software is done using SRTM DEM of 30 m spatial resolution and WorldView-1 Stereo DEM of 2 m spatial resolution, and the simulation of the whole event is performed using the RAMMS model having 10 m spatial resolution Cartosat data in the background. RAMMS: Debris Flow module is developed at the Swiss Institute for Snow and Avalanche Research and is designed for mass movement modelling phenomena which contain fast-moving particulate debris of rocks for realistic thermomechanical simulations.

## RESULTS

### Triggering of the Coalescent Natural Disaster

Initially, between 03-05 February 2021, the Dhauliganga River region received heavy snowfall (Fig. 3), which overloaded high, vulnerable, very steep slopes and in the morning of 07 February 2021, a north-facing triangular-shaped slope failed, which was also supporting a small hanging glacier. This has been assessed through time series of high spatial resolution remote sensing images of various satellites. The meteorological variables, e.g., air temperature, surface temperature, turbulent heat flux, radiative fluxes, heat and momentum transfer coefficients, specific humidity and upper wind patterns, were found to show significant departures from their usual patterns starting from 72 h until a few hours before the rock-ice avalanche event mentioned by (Srivastava et al., 2022) using Weather Research and Forecasting (WRF) model. A similar pattern was observed in the parameters downloaded from https://power.larc.nasa.gov/data-access-viewer and then the graph was plotted (Fig. 4). The average 2 m air temperature and land surface temperature near the avalanche site during the 48 h before the event were found to be much lower than the average temperatures post-event. The solar flux mostly remained downward (negative) in the 72 h before the event and was found to have an exceptionally large negative value a few hours before the rock-ice avalanche event. The part of the Himalayan region falling in the simulation domain received a significant amount of rainfall on 4 February, around 48 h prior to the event, while the rest of the days pre- and post-event were mostly dry. The data (Fig. 3) and graph (Fig. 4) presented here suggest the identification of the possible trigger factors of the event.

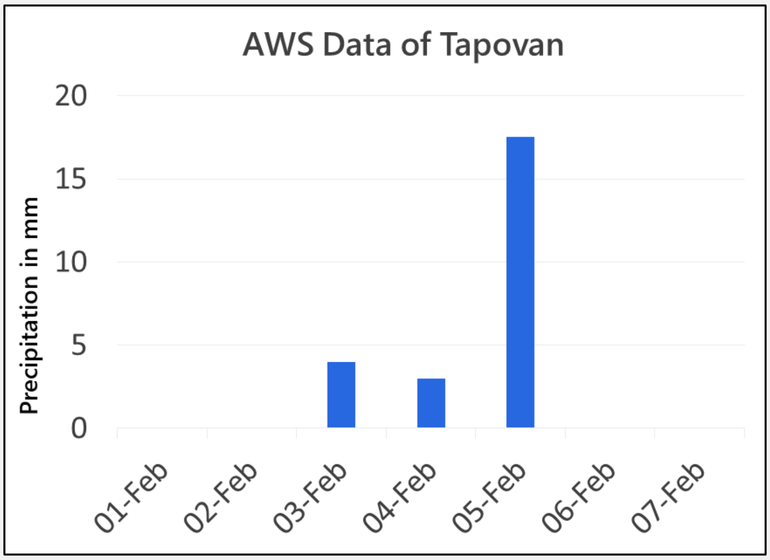

Figure 3. Total precipitation (snow and rain) occurred in the region. Data recorded at Automatic Weather Station, Tapovan)

The failure of the north-facing triangular-shaped slope and, consequently, massive debris flow into the Raunthi Gadhera initially blocked the flow of Dhauliganga near Rini village, which later failed around 10:15 hrs (local time) on 07 February 2021 and brought a catastrophic flash flood in the Dhauliganga river. It is important to note that there is no information about the exact timing of triangular-shaped slope failure due to the lack of availability of regular time series high spatial resolution satellite images. However, analysis of two images from different satellites revealed that just before 10:33 hrs. (local time) on 07 February 2021, a huge dust cloud in the Raunthi Gadhera was observed, and another satellite was observed image at 10:58 hrs. On the same day, that dust cloud moved towards Rishiganga and Dhauliganga valleys (Fig. 5). Shugar et al. (2021) also reported the movement of a dust cloud PlanetScope imagery from 5:01 UTC and 5:28 UTC on 7 February (10:31 and 10:58 IST).

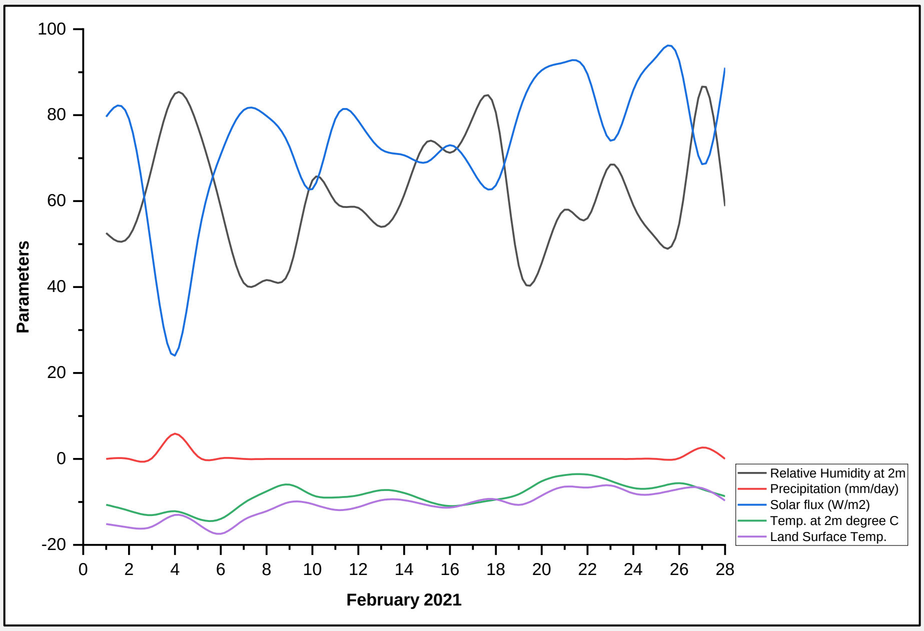

Figure 4. Graph showing deviation in relative humidity, average 2 m air and surface temperatures, solar flux and precipitation near the avalanche site before the event

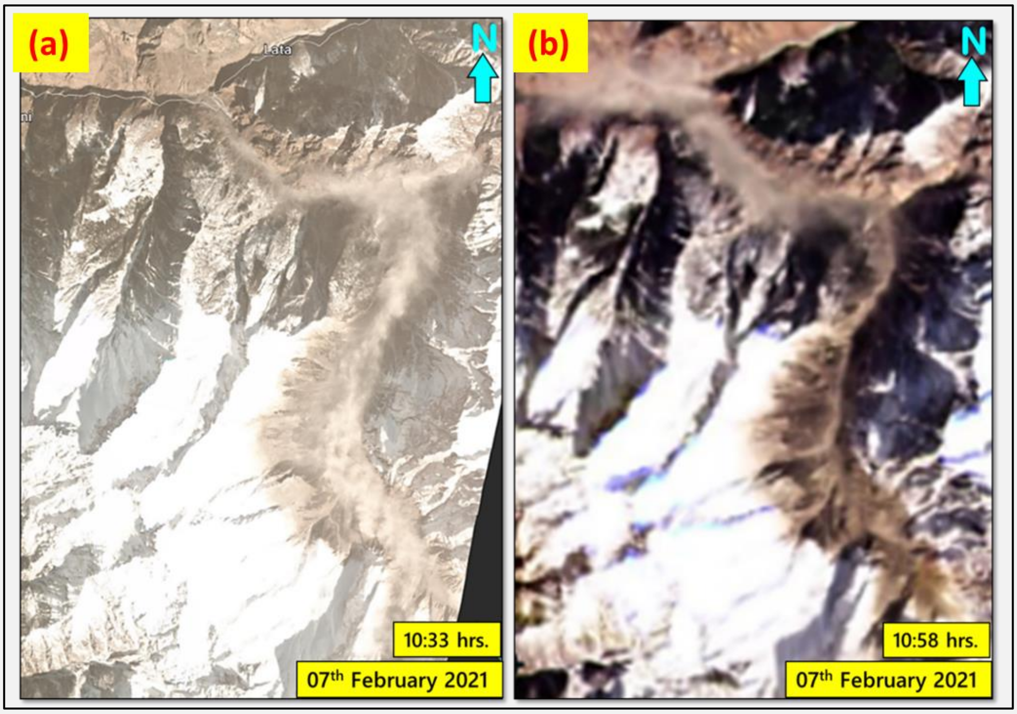

Figure 5. Satellite images of 07 February 2021 Left image (a) was acquired at 10:33 hrs (local time), and at 10:58 hrs later, the right image (b) was acquired. A comparison between (a) and (b) clearly deciphers the movement of the dust cloud towards downstream valleys, which also indicates that perhaps dust particles were moist and heavy and, in the absence of wind, settled naturally

In the present study, it has been further investigated to assess changes that occurred before and after the 07 February 2021 flash flood event by employing (i) high-resolution images of 06 February 2021 and 07 February 2021 of Pléiades satellite and (ii) a change detection pseudo colour transformation (PCT) technique developed by Saraf (1998). The conventional PCT technique facilitates the combination of various bands in different colour schemes, such as RGB, IHS and CMY. However, instead of using the different bands of the same date data, an approach developed by Saraf (1998) has been adopted in the present study to map the landslides/rockslide-induced ground changes using available high-resolution pre- and post-event datasets of Pléiades satellite. Both pre-and post-event Pléiades scenes were georeferenced using an image-to-image rectification technique. Since the available Pléiades images were in false colour composite (FCC) format and therefore first splitting of FCCs was done into their original colour components, i.e. red, green and blue (RGB), the pre-earthquake scene is kept in the red channel and the post-earthquake scene in the green and blue channels (Fig. 6). This has provided a change index with red depicting positive change in terms of reflectance between two dates, blue and green depicting negative change, and black and white depicting no change.

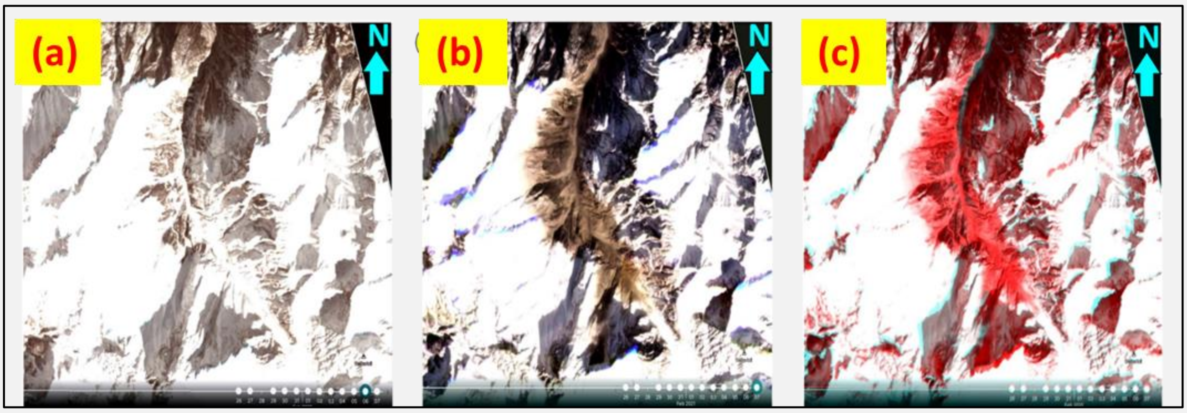

Figure 6. Pre-event Pléiades image of 06 February 2021 (a); Pléiades image of 07 February 2021, just after the rockslide event (b); Pseudo Colour Transformed (PCT) image of Band 3 (c) depicts changes (in red colour) that occurred between 06-07 February 2021 images. White areas decipher no changes. Cyan-coloured areas in PCT image (c) are due to differential shadows between images (a) and (b). Dust clouds in (c) along Raunthi Gadhera can be seen very evidently in red colour

### Area and volume estimation of triangular-shaped failed slope

High spatial resolution satellite images and later Google Earth images (including in background digital elevation model of the same) of the Dhauliganga disaster event, it has been possible to estimate the area and volume of the triangular-shaped failed slope. Based on various data sets and limited field inputs, the area of the triangle has been estimated to equal about 363000 $m^2$ (considering 660 m base and about 1100 m height of the facet). If an average thickness is considered to be 50 m (maximum being about 150 m) (Fig. 7), thus total estimated volume would be about 20 million $m^3$ (which includes rocks, snow and ice) (Fig. 8).

### Damming and Debris Flow

Rapid and colossal glacial debris flow into the Raunthi Gadhera initially blocked the flow of Dhauliganga near Rini village, which later failed around 10:30 hrs (local time) on 07 February 2021 and brought a calamitous flash flood in the Dhauliganga River, which killed 79 people and about 125 people are still missing. Due to the heavy flow of moraine sediments, both Rishiganga and Dhauliganga rivers were blocked. However, as clearly evident in post-event satellite images, natural damming at the Dhauliganga River near Rini village broke around 10:30 hrs (Fig. 9) on the same day and caused a devastating flash flood in the Dhauliganga River, damaging structures which came along the path of the river within a few minutes time even beyond Vishnuprayag town (Fig. 10).

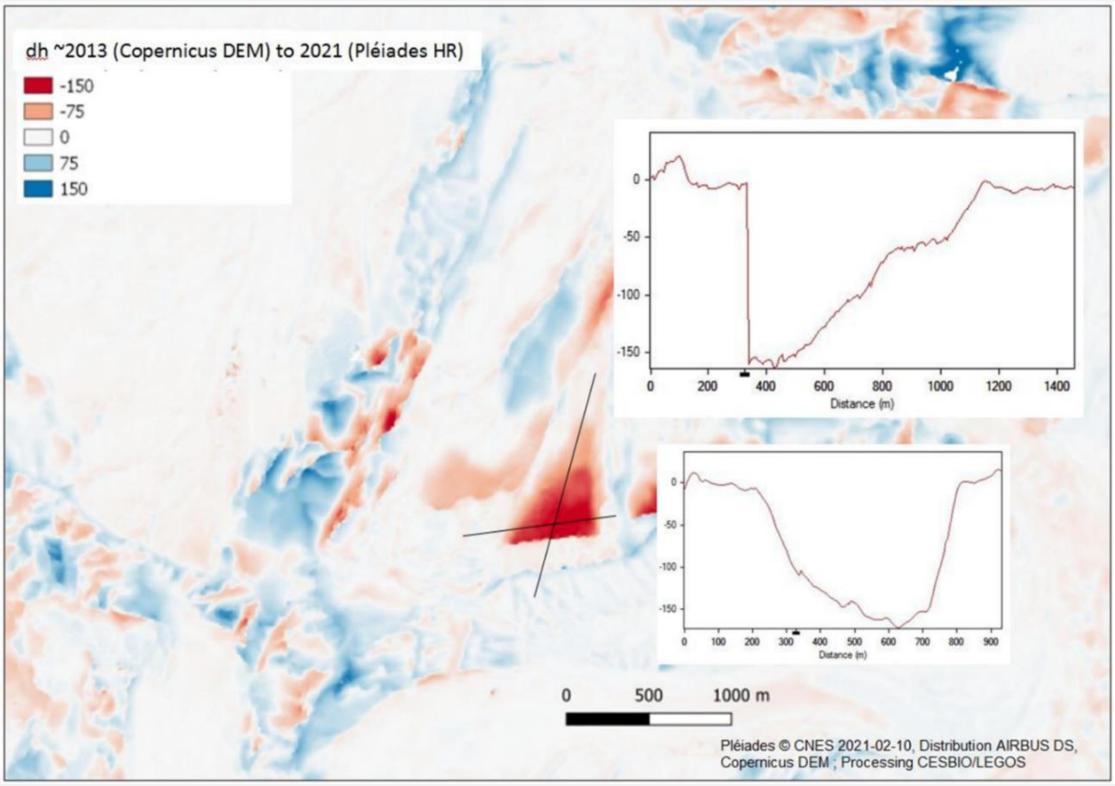

Figure 7. Area and volume estimation of triangular-shaped failed slope based on analysis of high spatial resolution 10 February 2021 Pléiades DEM and Copernicus 30 m DEM of 2013. Both along the slope and across slope profiles depicts a maximum depth of about 150 m *(Source*: Pléiades images of the Uttarakhand disaster, 2021)

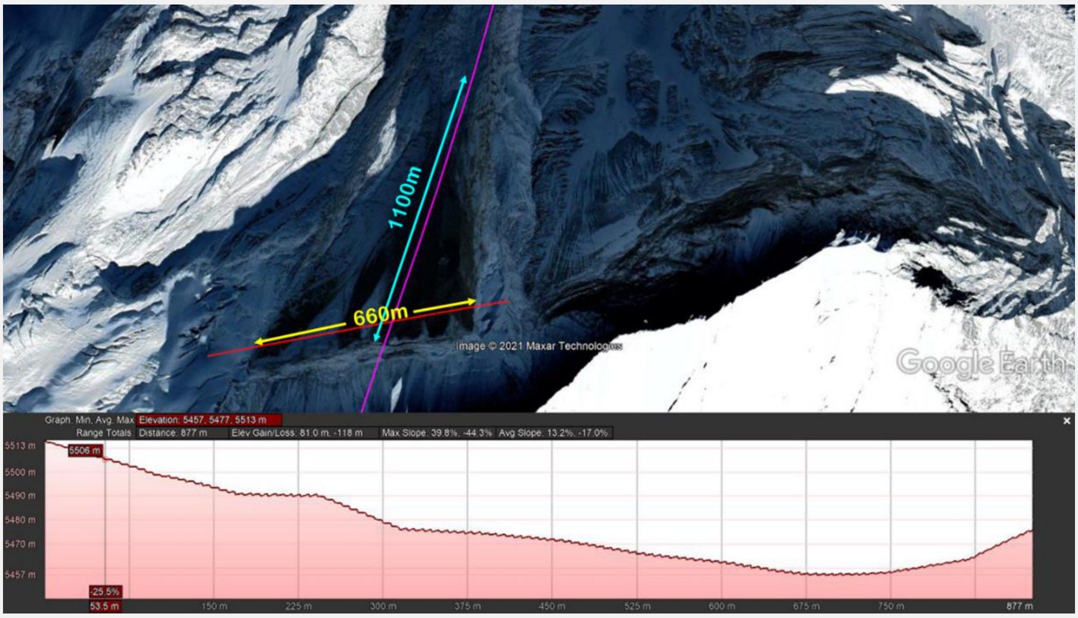

Figure 8. Dimensions of triangular-shaped failed slope as estimated employing Google Earth datasets (both high-resolution image and digital elevation model in the background). Across slope topographic profile (red coloured line with 660 m width as annotation). The topographic profile (bottom Figure) depicts the depth of the failed slope before the event

Figure 9. Google Earth image of 10 February 2021 brings a remnant of the broken natural dam, which can be realised clearly across the Dhauliganga River. As can be seen that heavy and abrupt moraine sediments (initially Rishiganga brought dark grey sediments as can be seen on both banks of Rishiganga River, and later it brought light grey sediments) were brought by the Rishiganga which initially blocked the flow of Dhauliganga. However, due to heavy flow in the Rishiganga, the temporary natural dam could not sustain and broke quickly, causing a devastating flash flood in the downstream stretch of Rishiganga

Figure 10. Image showing the debris flow along the path of Dhauliganga River, which completely destroyed the structures coming on the way
(Source: https://images.assettype.com/swarajya%2F2021-02%2Fd3a5cb91-ae7b-4fd2-b8ca-179e69a9ed02%2Fchamoli.png?w=480&q=75&auto=format%2Ccompress)

### Size and volume estimation of Rini's newly formed lake

After the catastrophic flash flood of 07 February 2021, an elongated lake was created due to the blocking of the flow of the Rishi Ganga River. This water impoundment can be seen very clearly on the Planet (Skysat-4) satellite image of 23 February 2021 (Fig. 11). The Planet (Skysat-4) image of 23 February 2021 evidently shows the elongated shape of the lake. Therefore, it is easy to map the size of the lake (length about 880 m, width at the front about 103 m). The average width of the lake can be estimated to be about 59 m, and therefore, the area of the lake would be about 25,000 m$^2$. Further, based on limited field data, the average depth of the lake can be taken at about 36 m (excluding freshly deposited debris and silt of about 10 m), and an estimated total volume of water in the lake might be ≈ 900000 m$^3$. However, the authorities worked to drain the lake to prevent any further flooding in the downstream areas, and it was eventually drained by early April 2021. The mention of this lake and its volume estimation is made by different scientists (Martha et al., 2021; Rana et al., 2021; Shugar et al., 2021), but none of them have done the simulation of the lake to know the actual volume.

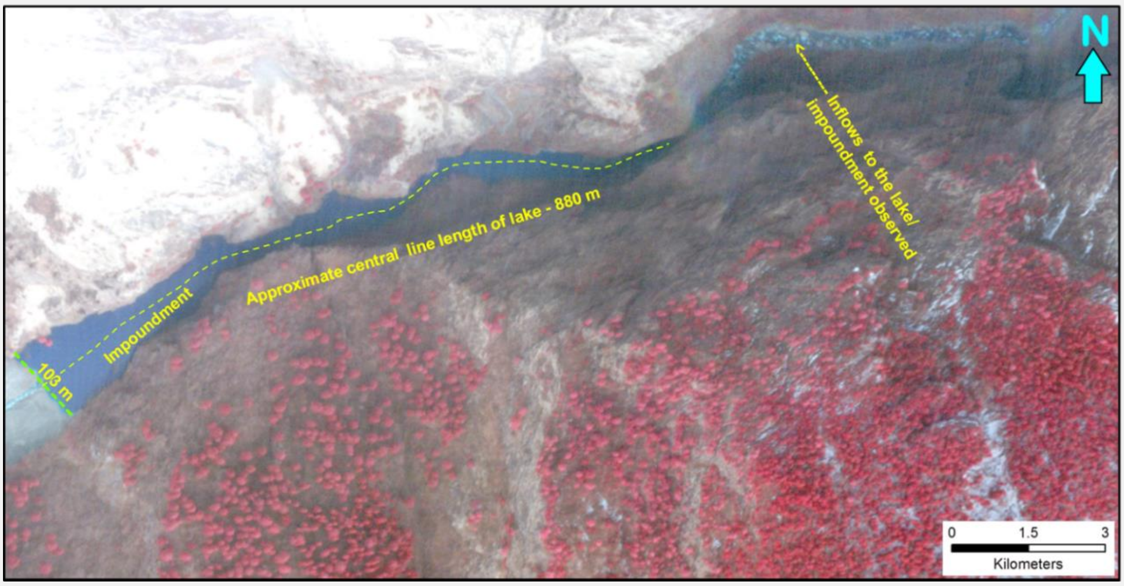

Figure 11. Planet (Skysat-4) image of 23 February 2021 depicts a newly formed lake on the Rishiganga River near Rini Village (NRSC, 2021b). A large and sudden supply of moraine debris due to rockslide/landslide blocked the Rishiganga River on 07 February 2021. It is important to note that the lake was formed on 07 February 2021 during the flash flood event; however, due to complete shadow conditions in the area, the lake was not clearly seen till 23 February 2021 (*Source*: NRSC, 2021b)

In order to evaluate the accurate volume of the lake, dam simulation technique in Geographic Information Systems (ArcView GIS and Profile Extractor extension) was employed in which SRTM (Shuttle Radar Topography Mission) DEM of 30 m spatial resolution and WorldView-1 Stereo DEM of 2 m spatial resolution have been used (Fig. 12). The actual volume of the lake obtained after the dam simulation using the two DEM came out to be lower than the estimated above using satellite image, i.e., around 5 million cubic meters (≈500000 m$^3$).

### Damage assessment

The two run-of-river hydroelectric power Rishiganga Small Hydro (13.2 MW) at 1975 m above MSL and Tapovan Vishnugad (520 MW) at 1795 m above MSL projects which were also severely damaged due to the devastating flash flood (Figs. 13, 14 and 15). More than 150 workers were trapped in the under-construction power tunnel (Fig. 14) of the Tapovan Vishnugad project. A visual comparison of images and field photographs is shown in Figs. 14 and 15 emphatically bring the extensive damages caused by the flash flood, which were caused in a few minutes. The damage to all kinds of structures along the Rishiganga-Dhauliganga Rivers runs beyond these project sites. In fact, any structure along these rivers was completely destroyed within a few minutes time even beyond Vishnuprayag town.

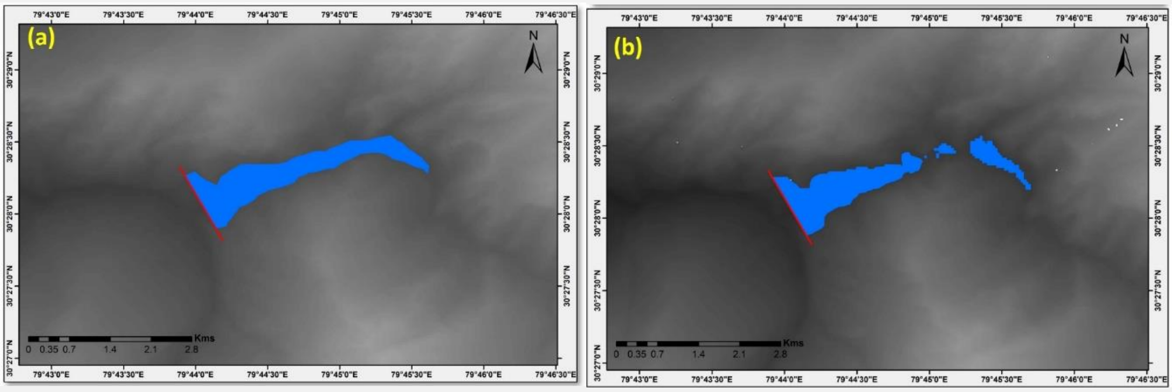

Figure 12. Simulated Reni Lake at 2600 m elevation with a dam axis of 1057 m from SRTM DEM of 30 m spatial resolution (a); Simulated Reni Lake at 2600 m elevation with a dam axis of 1057 m from WorldView-1 Stereo DEM of 2 m spatial resolution (b)

Figure 13. Pre- and post-event Google Earth images of the Rishiganga Hydro Power Project (13.2 MW) clearly show a complete washout of the operational hydropower project due to the devastating flash flood of 07 February 2021

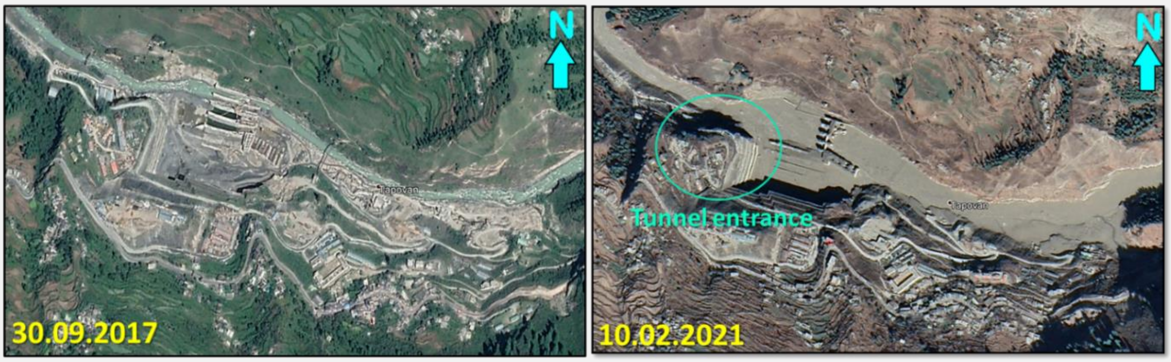

Figure 14. Pre- and post-event Google Earth images of Tapovan Vishnugad Hydro Power Project (520 MW) clearly show severe damage to the under-construction hydropower project due to the devastating flash flood of 07 February 2021

Figure 15. Before and after flash flood conditions of Tapovan Vishnugad Hydro Power Project (520 MW) clearly show severe damage to the under-construction hydropower project due to the devastating flash flood of 07 February 2021 (*Source*: Before - http://webtag.ae/rithwik/view/front/modules_/portfolio/data/27/hURCWLUssu3q.JPG After - https://static.toiimg.com/thumb/msid-80738861,width-1200,height-900,resizemode-4/.jpg)

### Simulation of the Event

The flow depth and flow velocity were modelled with the RAMMS (rapid mass movement simulation). Release Area and Calculation Domain were defined, where the release area is the amount of mass that came out in the form of debris, and the calculation domain is the area that got affected due to debris flow. In this modelling approach, the total volume of rock and ice has been estimated at about 20 million m$^3$ involving 10 m spatial resolution Cartosat DEM. This model clearly brings insight into the flow depth and upslope entry of sediments into the Rishiganga and Dhauliganga Rivers, which blocked the flow of water and created temporary dams (Fig. 16). The debris flow runout analysis showed that debris flow hit the valley with a ~220 m height (Fig. 16a) with a maximum velocity flow of ~74 m/s (Fig. 16b) and a maximum pressure of ~1097 kPa (Fig. 16c). The simulation was also performed by Sattar (2021) using ALOS PALSAR DEM having a spatial resolution of 12.5 m and calculated the volume as 25 million m$^3$ (20 million m$^3$ of rock and 5 million m$^3$ of ice).

## DISCUSSION

Rishiganga Valley lies in the central Himalayas, and these young mountains are structurally very fragile and also exposed to the extreme climatic conditions prevalent in the region. Before the occurrence of the flash floods on February 2021, a similar type of event was observed in the month of September-October 2016. However, this event did not get much attention as there was no loss of life or property involved. The time series images clearly reveal such ice avalanche breakoff, which brought moraine deposits along Raunthi Gadhera (Fig. 18). Fig. 17(c) image of 07 October 2017 further conveys evidence of breakoff of ice and rocks and bringing additional sediments in the Raunthi Gadhera, which visibly specifies that there were continuous such activities in that area. Later, the same area (just east of the September-October 2016 area) (Fig. 17) broke out and caused the coalescent natural disaster of 07 February 2021.

It is stimulating to note that the ice avalanche breakoff/rockslide moraine sediments do not stay long in the Raunthi Gadhera. Time series images shown by GAPHAZ (2021) (Fig. 18) emphatically show that in 3-4 years' time, the monsoon rains in the area can flush out such sediments. Such rapid flushing of sediments from the streams also indicates that the sediments deposited due to the 07 February 2021 events will also flush out soon. However, comparatively, the latest event has deposited more sediments not only in the Raunthi Gadhera but also along Rishiganga and Dhauliganga Rivers. Inevitable heavy rains in the coming Monsoon seasons will be flushing out the newly deposited debris from these streams, which may become the source of various other problems in the downstream areas.

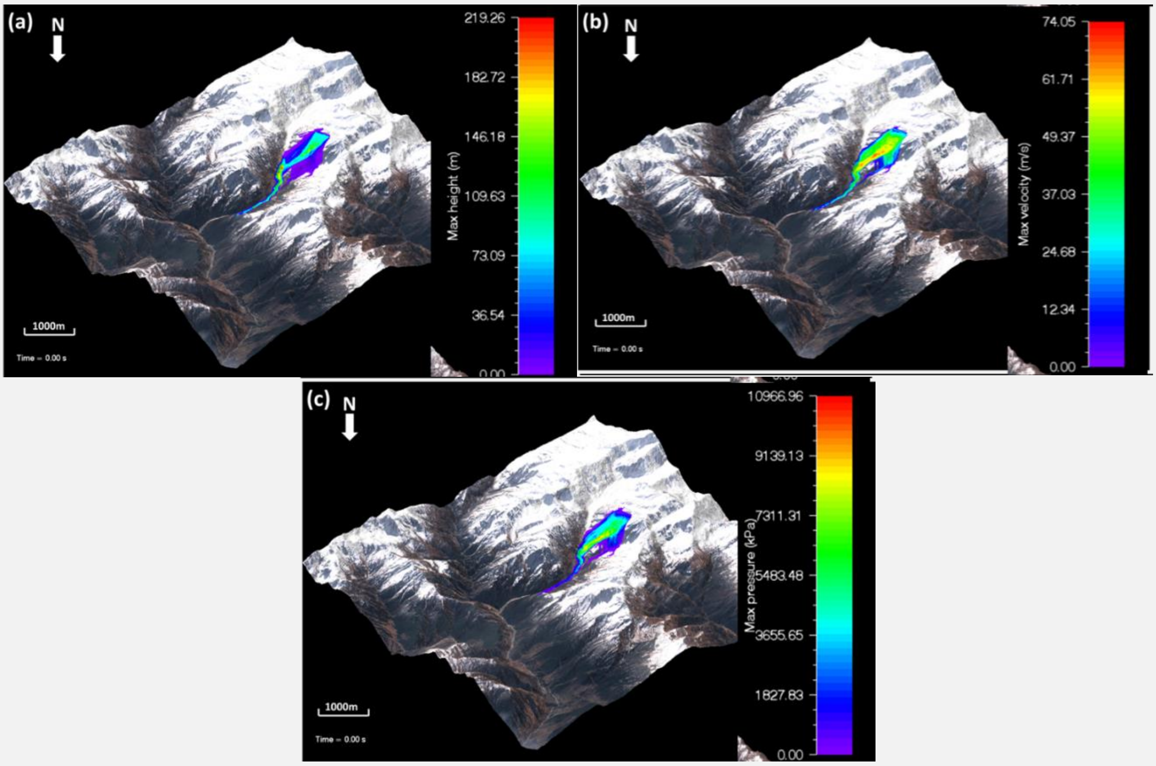

Figure 16. Reconstruction of flow depth and flow velocity with the RAMMS model for an assumed 20 million m$^3$ rock and ice avalanche showing max. height (a); max. velocity (b); and max. pressure (c)

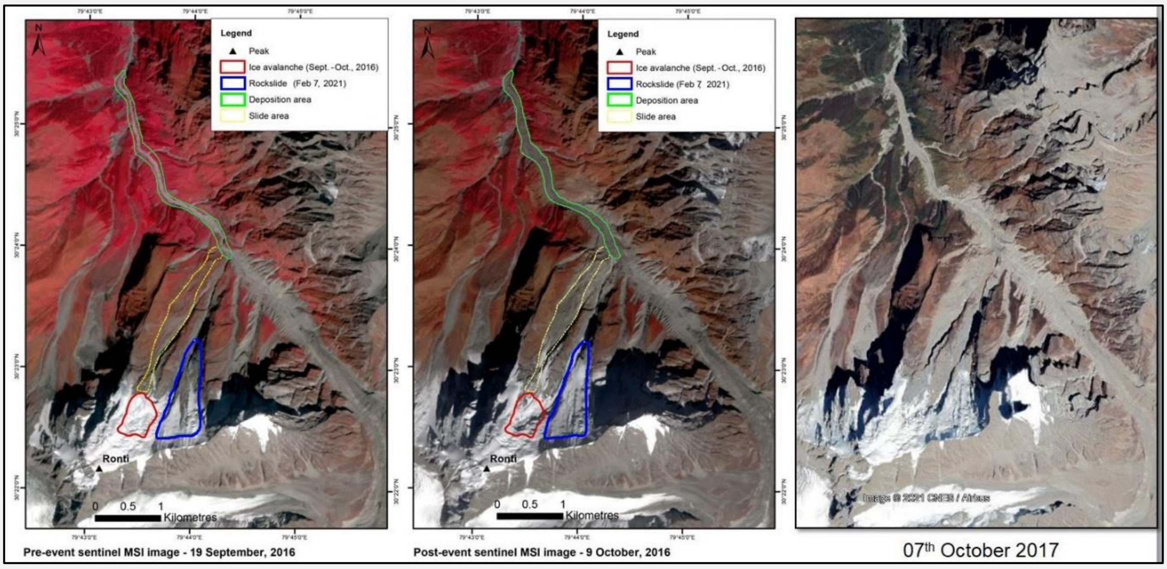

Figure 17. The ice avalanche breakoff between 19 September and 9 October 2016 (solid red outline) with the area covered by resulting moraine deposits along the Raunthi Gadhera (green line) and flow surface (dotted yellow line). The blue outline shows the present rockslide scarp (after Shrestha et al., 2021). Image (c) of 07 October 2017 further reveals that there were continuous activities of breaking off rocks and additional deposition of sediments in the Raunthi Gadhera valley (*Source:* Shrestha et al. 2021)

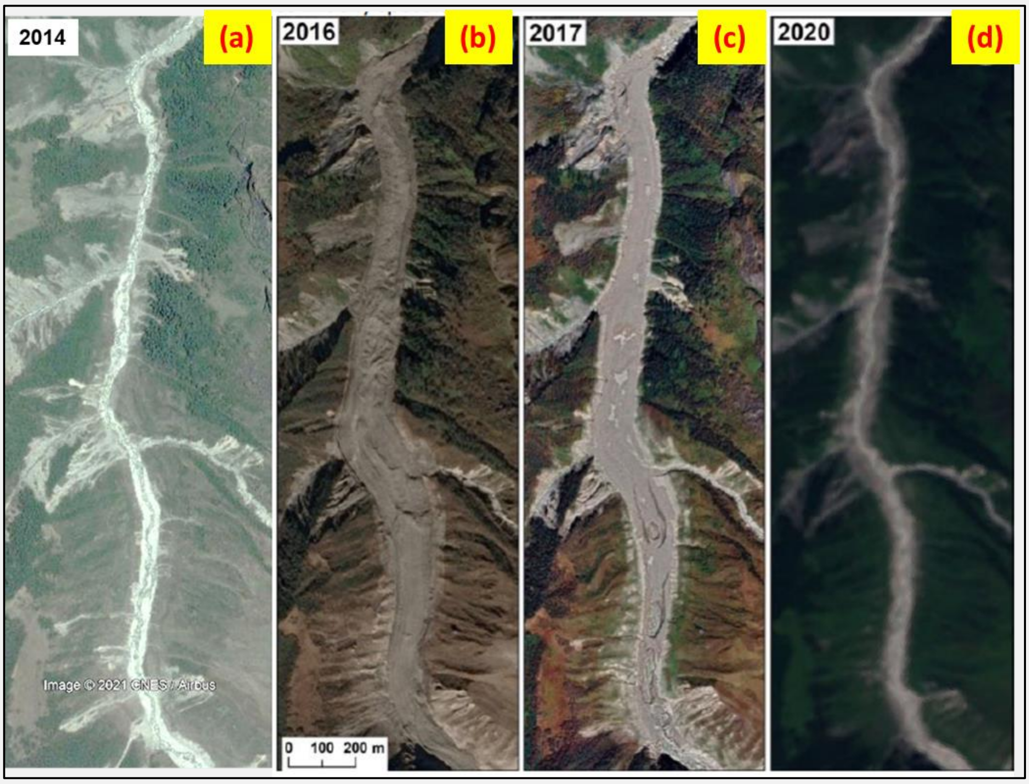

Figure 18. Moraine deposits of the September-October 2016 ice avalanche from the neighbouring glacier. 2020 pre-event Sentinel-2 image (d) indicates the normal flow of the river, similar to the Google Earth image of 2014 (a). The debris-covered ice, visible in the (b) and central panel (c) from 2016 and 2017, seems to have disappeared in the year 2020, much before the 2021 avalanche (GAPAZ, 2021)

Sarkar & Saraf (2000), Saraf et al. (2009), Sharma et al. (2018) have evidently demonstrated that there are generally early signatures of slope failure. Any triggering factor, e.g. heavy precipitation, an earthquake, anthropogenic activities etc., can fail such vulnerable slopes, as happened in the present study area (just below Ronti Peak, the origin of Raunthi Gadhera); a triangular-shaped slope could not sustain heavy and swift snow overloading. Time series satellite images undoubtedly depict that there was the early signature of slope failure (Fig. 19). Comparison of both images [(a) and (b) images of Fig. 19] clearly establishes the fact of early signs of slope failure. And moreover, these cracks were visible from the year 2017 itself, which might have developed after the ice avalanche break off during the past event which happened in September-October 2016 (Fig. 20). Here, it is important that if regular monitoring had been employed, then perhaps loss of life could have been completely avoided.

## CONCLUSION

This study presents a detailed analysis of the coalescent natural disaster and its sequence of events. Based on the study, several key findings were obtained. Firstly, the triangular-shaped failed slope had a base of 660 m and a height of about 1100 m, resulting in an estimated area of approximately 363000 $m^2$. Secondly, the RAMMS model was used to reconstruct the flow depth and velocity, assuming a volume of 20 million $m^3$, which included rock and ice avalanche. Thirdly, the volume of the Rini Lake, after simulating the dam, was found to be lower than the estimated value obtained using satellite images, approximately 5 million cubic meters (≈500000 $m^3$). Fourthly, the study emphasized the importance of high-resolution time series satellite images and the application of GIS to assess damages and estimate parameters associated with slope failures and lake formation. Additionally, automatic/semi-automatic change detection algorithms and software tools could be developed to detect even minuscule changes in vulnerable areas and provide long-term/short-term forecasts of similar events. However, the study also identified limitations in volume calculation done by simulation models using the digital elevation model as input, as the type of DEM used can affect the results, although the variations are minimal.

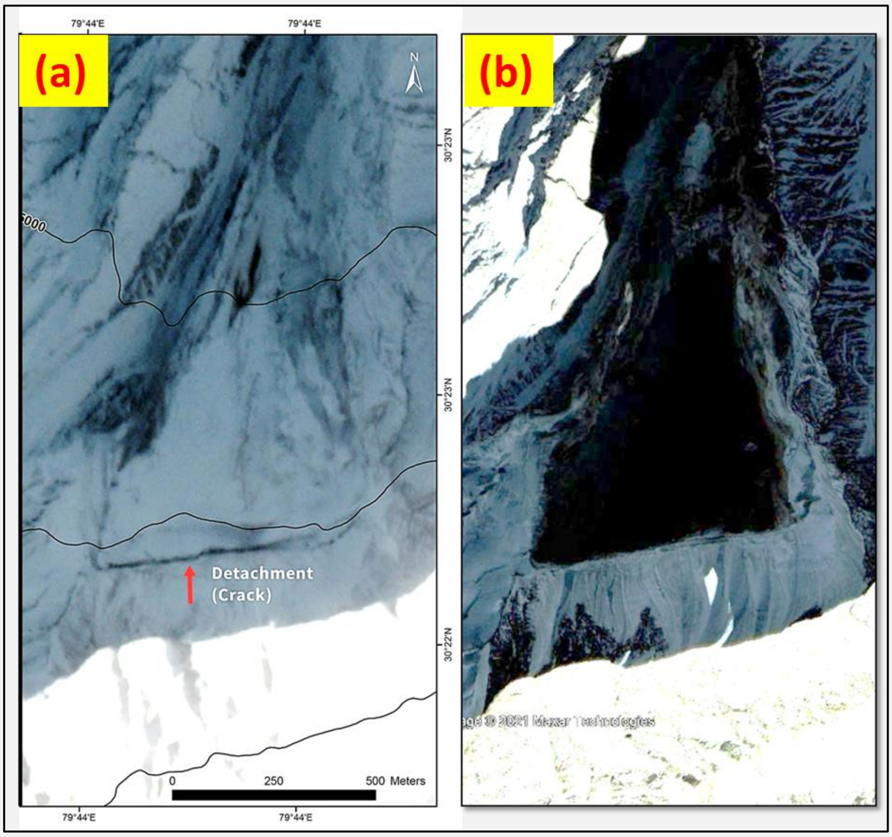

Figure 19. Sentinel-2A image of 06 February 2021 (a) Google Earth image of 10 February 2021 (b) Evidently, a detachment crack can be seen in the left image (marked with a red arrow) just one day before the event. Further, thick snow on 06 February can also be seen in image (a) Comparison of both images clearly demonstrates once again that there are early signatures of slope failure

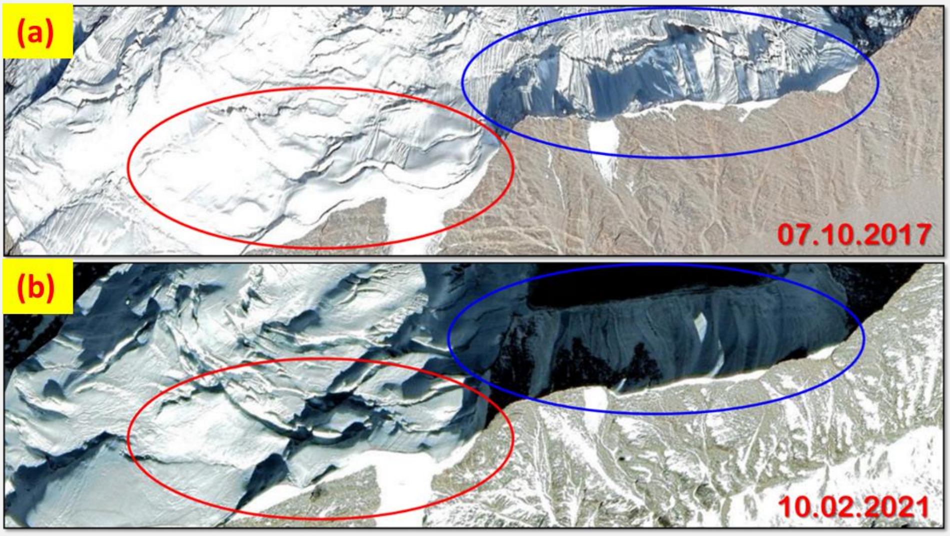

Figure 20. Google Earth images of 07 October 2017 (a) and 10 February 2021 (b). Developments of cracks can be seen (blue ellipse) emphatically indicating imminent possibilities of slope failures, which really happened on 07 February 2021 (also seen in Fig. 11). The red ellipse is now indicating future slope failures, which may be triggered due to heavy snow/rains as happened in the neighbouring areas during February 2021 which brought devastating coalescent disaster in the downstream areas.

## ACKNOWLEDGEMENT

The note is a voluntary effort of the authors, and it includes their independent opinion other than synthesised materials and information, which is gratefully acknowledged. This is a very preliminary and brief analysis based on the presentation of available data, images, and information. We will do more technical analysis in our future endeavours and update our notes accordingly.

## SUPPLEMENTARY MATERIAL

The simulated Graphics Interchange Format (.gif) files for the simulation of the event can be downloaded from https://drive.google.com/file/d/1jZvm_Tw-Wkr5tZnwtdePxNYanR4FhpNV/view?usp=share_link

## REFERENCES

Allen, S. K., Cox, S. C., & Owens, I. F. (2011). Rock avalanches and other landslides in the central Southern Alps of New Zealand: A regional study considering possible climate change impacts. *Landslides*, *8*(1), 33–48. https://doi.org/10.1007/s10346-010-0222-z

Batar, A. K., & Watanabe, T. (2021). Landslide susceptibility mapping and assessment using geospatial platforms and weights of evidence (WoE) method in the Indian Himalayan Region: recent developments, gaps, and future directions. *ISPRS International Journal of Geo-Information*, *10*(3), 114. https://doi.org/10.3390/ijgi10030114

Davies, M. C. R., Hamza, O., & Harris, C. (2001). The effect of rise in mean annual temperature on the stability of rock slopes containing ice-filled discontinuities. *Permafrost and Periglacial Processes*, *12*(1), 137–144. https://doi.org/10.1002/ppp.378

Dwivedi, D. K., Saraf, A. K., & Das, J. D. (2023). Geoinformatics-based investigation of slope failure and landslide damming of chenab river, lahaul-spiti, Himachal Pradesh, India. *Natural Hazard Research*. https://doi.org/10.1016/j.nhres.2023.02.008

Evans, S. G., & Clague, J. J. (1994). Recent climatic change and catastrophic geomorphic processes in mountain environments. *Geomorphology*, *10*(1–4), 107–128. https://doi.org/10.1016/0169-555X(94)90011-6

Fischer, L., Purves, R. S., Huggel, C., Noetzli, J., & Haeberli, W. (2012). On the influence of topographic, geological and cryospheric factors on rock avalanches and rockfalls in high-mountain areas. *Natural Hazards and Earth System Science*, *12*(1), 241–254. https://doi.org/10.5194/nhess-12-241-2012

Geertsema, M., Clague, J. J., Schwab, J. W., & Evans, S. G. (2006). An overview of recent large catastrophic landslides in northern British Columbia, Canada. *Engineering Geology*, *83*(1–3), 120–143. https://doi.org/10.1016/j.enggeo.2005.06.028

Haeberli, W., Wegmann, M., & Mühll, D. V. (1997). Slope stability problems related to glacier shrinkage and permafrost degradation in the Alps. *Eclogae Geologicae Helvetiae*, *90*(3), 407–414. http://doi.org/10.5169/seals-168172

Kala, C. P. (2011). Save Ganga campaign and hydroelectric projects in Uttarakhand. *Current Science*, *101*(5), 596.

Kala, C. P. (2014). International Journal of Disaster Risk Reduction Deluge , disaster and development in Uttarakhand Himalayan region of India : Challenges and lessons for disaster management. *International Journal of Disaster Risk Reduction*, *8*, 143–152. https://doi.org/10.1016/j.ijdrr.2014.03.002

Martha, T. R., Roy, P., Jain, N., Vinod Kumar, K., Reddy, P. S., Nalini, J., Sharma, S. V. S. P., Shukla, A. K., Durga Rao, K. H. V., Narender, B., Rao, P. V. N., & Muralikrishnan, S. (2021). Rock avalanche induced flash flood on 07 February 2021 in Uttarakhand, India—a photogeological reconstruction of the event. *Landslides, 18(*8), 2881-2893. https://doi.org/10.1007/s10346-021-01691-9

Meena, S. R., Mishra, B. K., & Tavakkoli Piralilou, S. (2019). A hybrid spatial multi-criteria evaluation method for mapping landslide susceptible areas in kullu valley, himalayas. *Geosciences*, *9*(4), 156. https://doi.org/10.3390/geosciences9040156

Oppikofer, T., Jaboyedoff, M., & Keusen, H. R. (2008). Collapse at the eastern Eiger flank in the Swiss Alps. *Nature Geoscience*, *1*(8), 531–535. https://doi.org/10.1038/ngeo258

Pant, V., & Pande, P. R. K. (2012). Disaster Risk Analysis ( DRA ): Case Studies from Pithoragarh district, Uttarakhand, India. *IOSR Journal of Humanities and Social Science*, *1*(6), 24–26. http://dx.doi.org/10.9790/0837-0162426

Rana, N., Sharma, S., Sundriyal, Y., Kaushik, S., Pradhan, S., Tiwari, G., Khan, F., Sati, S. P., & Juyal, N. (2021). A preliminary assessment of the 07 February 2021 flashflood in lower Dhauli Ganga valley, Central Himalaya, India. *Journal of Earth System Science*, *130*(2). https://doi.org/10.1007/s12040-021-01608-z

Sangeeta, & Maheshwari, B. K. (2019). Earthquake-Induced Landslide Hazard Assessment of Chamoli District, Uttarakhand Using Relative Frequency Ratio Method. *Indian Geotechnical Journal*, *49*(1), 108–123. https://doi.org/10.1007/s40098-018-0334-2

Saraf, A. (1998). Assessing the causes and damages using remote sensing and GIS techniques. *GIS@Development*.

Saraf, A., Das, J., & Rawat, V. (2009). Satellite Based Detection of Early Occurring and Co-Seismic landslides. *Journal of South Asia Disaster Studies*, *2*, 47–55.

Sarkar, I., & Saraf, A. K. (2000). Some observations of the Chamoli earthquake-induced damage using ground and satellite data. *Current Science*, *78*(1), 91-97. https://www.jstor.org/stable/24103854

Sarkar, S., Roy, A. K., & Raha, P. (2016). Catena Deterministic approach for susceptibility assessment of shallow debris slide in the Darjeeling Himalayas , India. *Catena*, *142*, 36–46. https://doi.org/10.1016/j.catena.2016.02.009

Sattar, A. (2021). *First insights into the Chamoli disaster , 07 February 2021*. *2021*, 2–8.

Sharma, K., Saraf, A. K., Das, J., Baral, S. S., Borgohain, S., & Singh, G. (2018). Mapping and Change Detection Study of Nepal-2015 Earthquake Induced Landslides. *Journal of the Indian Society of Remote Sensing*, *46*(4), 605–615. https://doi.org/10.1007/s12524-017-0720-8

Shrestha, A. B., J Steiner, S. Nepal, S. B. Maharjan, M. Jackson, G. Rasul, and B. Bajracharya, (2021), *Understanding the Chamoli flood: Cause, process, impacts, and context of rapid infrastructure development*, https://www.icimod.org/article/understanding-the-chamoli-flood-cause-process-impacts-and-context-of-rapid-infrastructure-development/ (Accessed on 09 April 2021).

Shugar, D. H., Jacquemart, M., Shean, D., Bhushan, S., Upadhyay, K., Sattar, A., Schwanghart, W., McBride, S., de Vries, M. V. W., Mergili, M., Emmer, A., Deschamps-Berger, C., McDonnell, M., Bhambri, R., Allen, S., Berthier, E., Carrivick, J. L., Clague, J. J., Dokukin, M., … Westoby, M. J. (2021). A massive rock and ice avalanche caused the 2021 disaster at Chamoli, Indian Himalaya. *Science*, *373*(6552), 300–306. https://doi.org/10.1126/science.abh4455

Srivastava, P., Namdev, P., & Singh, P. K. (2022). 7 February Chamoli (Uttarakhand, India) Rock-Ice Avalanche Disaster: Model-Simulated Prevailing Meteorological Conditions. *Atmosphere*, *13*(2), 267. https://doi.org/10.3390/atmos13020267